

## muCooling of Electronic Components Using Nanofluids

M. Zitoune<sup>1,2</sup>, O. Ourrad Meziani<sup>2</sup>, B. Meziani<sup>2</sup> and M. Adnani<sup>1,2</sup>

**Abstract** A finite volume code used for detailed analysis of forced-convection flow in a horizontal channel containing eight heat sources simulating electronic components. The study deals the effect of variations of Reynolds number, the volume fraction and the good choice of type of nanoparticles added to the base fluid. The study shows that the rate of heat transfer increases with increasing Reynolds number and the volume fraction of nanofluids but not infinitely. The analysis of the dynamic and thermal field shows that the heat transfer is improved, with the increase in the Reynolds number and the volume fraction. The study also shows that the choice of nanoparticles added to the base fluid is crucial, otherwise the best cooling electronic components is observed when using copper nanoparticles followed by those of alumina trioxide.

**Keywords:** Forced convection, nanofluid, finite volume method, electronic components.

### Nomenclature

L	Channel length ( <b>m</b> )
H	Channel height ( <b>m</b> )
T	Temperature ( <b>k</b> )
P	pressure ( <b>Pa</b> )
K	Thermal conductivity ( <b>W m<sup>-1</sup> K<sup>-1</sup></b> )
C <sub>p</sub>	specific heat at constant pressure ( <b>J kg<sup>-1</sup> K<sup>-1</sup></b> )
q <sub>v</sub>	Volumetric heat generation ( <b>Wm<sup>-3</sup></b> )
S <sub>p</sub>	Distance between the two substrates ( <b>m</b> )
S <sub>b</sub>	Distance between two successive blocks ( <b>m</b> )
h <sub>p</sub>	Bloc thickness ( <b>m</b> )
W <sub>p</sub>	Bloc length ( <b>m</b> )
S <sub>bas</sub>	Distance between the low wall and the substrate( <b>m</b> )

---

<sup>1</sup>Laboratoire de Mécanique, Matériaux et Energétique, Université de Béjaïa, Campus de Targua Ouzemour, Béjaïa, 06000 –Algeria.

<sup>2</sup>Laboratoire de Physique Théorique, Université A. Mira de Bejaïa, Campus de Targua Ouzemour, 06000, Bejaïa, Algeria.

<sup>1</sup> Corresponding Author: Mounir Zitoune, E-mail: zitoune.mounir@yahoo.fr.

$S_{\text{haut}}$	Distance between the top wall and the substrate ( <b>m</b> )
$x, y$	Cartesian coordinates ( <b>m</b> )
$u, v$	Components of the velocity vector ( <b>ms<sup>-1</sup></b> )
$h$	Convective heat transfer coefficient ( <b>Wm<sup>-2</sup>K<sup>-1</sup></b> )
$u_0$	Inlet velocity ( <b>m/s</b> )
$T_0$	Inlet temperature ( <b>K</b> )

**Greek symbols**

$\mu$	Dynamic viscosity ( <b>pa/s</b> )
$\rho$	Mass density ( <b>Kgm<sup>-3</sup></b> )
$\alpha$	Thermal diffusivity ( <b>m/s<sup>2</sup></b> )
$\theta$	Temperature dimensionless
$\varphi$	Volume fraction of the nanoparticles
$\nu$	Kinematic viscosity ( <b>m<sup>2</sup>/s</b> )

**Subscript**

$b$	bloc
$nf$	nanofluid
$s$	solid
$p$	particle

**1 Introduction**

Heat transfer proposes to quantitatively describe the evolution of some characteristic quantities of system, especially temperature at an initial equilibrium state and a final equilibrium state. It manifests in three modes (conduction, convection and radiation). The three modes of heat transfer occur simultaneously, most of the time, in the practical problems. The efforts to improve heat exchange in many industrial sectors, require the intensification of heat transfer by convection or conduction. The improvements in the exchange surfaces are widely explored and attaining its limits, and the air cooling was the most widely used method of cooling electronic components because it is easy to incorporate and is cheaply available, But With emergence and development of Nano sciences and Nanotechnologies in the second half of the 20th century, the convection has been taking much of this development. Furthermore, in the Nano metric level of the material of the convective medium that recent works has been concentrated. The basic idea is to increase the rate of heat transfer by introducing in a pure fluids a low concentration of nanoparticles. The term "Nano fluid" is introduced for the first time by [Choi (1995)]. The Nano fluids are fluids in which are inserted nanoparticles (diameter less than 100 nm). The synthesis of nanoparticles satisfies the need to improve the thermal diffusivity of liquid coolers by adding a solid phase which possesses a better thermal conductivity but does not sediment.

A great amount of experimental research in this field has recently been reported in

literature [Parametthanuwat, Bhuwakietkumjohn, Rittidech and Ding (2015)] report on an experimental investigation of the thermal properties behavior of the nanofluid (water+silver) with concentration of 0.5% , it was shown that the nanofluid with 1% yielded the highest thermal behavior enhancement of about 28% at 80 °C compared to deionized water. [Zhang, Hong, Wu, Liu, Xiao, Chen and Cheng (2014)] showed that suspension stability of the Carbon nanotubes-based nanofluids was greatly improved by surface modification of the carbon nanotubes; the thermal conductivity of the CCNTs-based nanofluids was further enhanced and became more stable by surface modification. [Khedkar, Sonawane and Wasewar (2013)] have studied experimentally the water to nanofluids heat transfer in concentric tube heat exchanger. They observed that, 3 % nanofluids shown optimum performance with overall heat transfer coefficient 16% higher than water. [Hussein, Bakar and Kadirgama (2014)] studied experimentally and numerically forced convection using (SiO<sub>2</sub>-water) as coolant in an automobile radiator. Four different volume concentrations of nanofluid from 1% to 2.5%. Reynolds number is of the order of 500 to 1750. The results showed that the friction coefficient decreases with increasing of the rate of flow and the volume concentration. The Nusselt number is proportional to the rate of flow, the volume concentration and the inlet temperature of nanofluid. It also showed that the use of SiO<sub>2</sub> with low concentration can increase the heat transfer rate up to 50% in comparison with pure water.

A considerable number of numerical researches and investigations were conducted on free, forced and mixed convection in different geometries with presence of a nanofluid. [Minea (2014)] studied numerically forced convection with a conventional fluid and a nanofluid in laminar regime, in a tube formed of both zones one is insulated and the other is submitted to a constant heat flux. The fluid enters within the tube with a constant inlet temperature of 300 K and a uniform axial velocity. The Reynolds number is between 500 and 2300. The second zone is subjected to a uniform heat flux of 10000 W/m<sup>2</sup>. therefore The results show that the heat transfer coefficient of Nano fluid increased from 3.4% to 27.8% compared to the pure water with a fixed Reynolds number(Re= 500). Which clearly shows that the nanoparticles suspends in the water improve the heat transfer by convection. [Yang and Lai (2010)] investigated the forced convection with the nanofluid (water-Al<sub>2</sub>O<sub>3</sub>) in a radial flow cooling system. A numerical simulations are performed basing of experimental work in the conditions with the following values: the diameter of nanoparticles d=47nm, the heat flux q=2438 and 3900 W/m<sup>2</sup> and a range of Reynolds number from 300 to 900. The results obtained for the overall performance of heat transfer with the Nano fluid indicate that the heat transfer coefficient is proportional to the Reynolds number and the volume fraction of the nanoparticles. [Elmir, Mehdaoui and Mojtabi (2012)] studied numerically cooling a solar cell by forced convection in the presence of the Nanofluid (Al<sub>2</sub>O<sub>3</sub>-water). The inclined channel walls are adiabatic, the silicon solar cells are submitted to a constant temperature. The Nano fluid is introduced into the channel with a constant vertical velocity and ambient temperature. The effect of the volume fraction of nanoparticles for various values Reynolds Number is examined. The results obtained showed that the presence of nanoparticles in the fluid increases the heat transfer rate in comparison with the base fluid, by enhancing the cooling of solar cells and therefore a good performance of the solar panel. [Hajipour and Dekhordi (2014)] studied mixed convection inside a rectangular channel submitted to a constant heat flux,

and partially filled with a metal foam. The study is performed with different volume concentration of alumina. The velocity and temperature profiles were obtained by using the finite difference method. The Brownian effects of nanoparticles were considered in the governing equations and the assumption of local thermal equilibrium was considered for solid and liquid phases. Finally the experimental results are in good agreement with the numerical results. [Mahmoudi, Shahi and Talebi (2010)] have studied numerically a mixed convection in a square cavity in the presence of nanofluid (copper water). In order To study the effect of the location of the input and output, four different configurations were considered. The study was conducted for different Reynolds numbers ranging from 50 up to 1000, Richardson number from 0 to 10, and a volume fraction of from 0 to 0.05. The results showed that the smallest and the largest heat transfer rate are obtained for the cases where the output and the input of cavity are both on the top and bottom respectively, and that for a high number of Richardson, the presence of the nanoparticles is more effective in case where the input is in the bottom and the output is the top of cavity in comparison with other configurations. In a similar numerical analysis, on the mixed convection [Mehrizi, Farhadi, Afroozi, Sedighi and Darz (2012)] have studied the effect of different nanoparticles and the effect of the position of the outlet on the heat transfer rate in a square cavity with one input and three output, where an isothermal hot obstacle is placed in the center of geometry. The study was conducted for  $0.1 \leq Ri \leq 10$ ,  $Gr=10^4$  and a volume fraction ranging from 0 to 0.03. The results indicate a maximum heat transfer rate were obtained when the output is set in the middle for  $Ri=0.1$  and in the top for  $Ri=1$  and  $Ri=10$ , respectively. It also rises by increasing the volume concentration of the nanoparticles in different numbers of Richardson and outlet positions. [Shahi, Mahmoudi and Talebi (2009)] have made a numerical research on mixed convection in a square cavity with one input and output using a nanofluid (Cu-water), the lower wall is subjected to a flux constant heat. The study was carried out by varying the Reynolds number in the range of  $50 \leq Re \leq 1000$ , the Richardson number in the range of  $0 \leq Ri \leq 10$  and the volume fraction in the range of  $0 \leq \phi \leq 0.05$ . The results indicate that increasing the concentration of the nanoparticles leads to the increase in the average Nusselt number and to reduce the average temperature. [Akbari, Behzadmehr and Shahraki (2008)] have made a comparative study with preceding numerical work on the laminar mixed convection of a nanofluid ( $Al_2O_3$ -water) in a horizontal and inclined tube. They found a good agreement, noting that the concentration of the nanoparticles do not have significant effects on the hydrodynamic parameters, the friction coefficient increases continuously with increasing inclination of the tube, and the transfer coefficient heat reaches the maximum at the angle of inclination of  $45^\circ$ . [Kherbeet, Mohammed and Salman (2012)] have investigated the effect of the variation of nanofluids on the heat transfer in a horizontal channel with a downward step by heating the descending wall, using different types of nanoparticles of diameter  $D$  between 25 and 70 nm, and volume fractions ranging from 1 to 4%. They found that nanofluids have the lowest density, have the highest rate in the same section. The results also indicated that the Nusselt number increases by increasing the volume fraction and nanoparticle size. [Izadi, Behzadmehr and Jalali-Vahida (2009)] have studied numerically forced convection in laminar flow by introducing a nanofluid consisting of  $Al_2O_3$  and water. The single-phase approach is used for modeling the nanofluid. They studied the axial variation of the temperature and

velocity, and the variation of heat transfer coefficients and friction at the area of the inner and outer walls. The results obtained show that the axial velocity profile does not change significantly with the volume fraction of the nanoparticles, but the temperature profiles are affected by the concentration of the nanoparticles. On the other hand, the transfer coefficient increases with the concentration of the nanoparticles

It is obvious from the above literature review that the study of cooling enhancement of laminar forced convection flow using nanofluids in a channel containing heat source simulating electronic components with constant volumetric heat generation seems not to have been investigated in the past, and this has motivated the current work. The main aim of this study is to examine the effect of Reynolds number on the forced convective flow and temperature field and chose the best nanoparticles to add to the base fluid (i.e. pure water) with the appropriate volume fraction in order to obtain an efficient cooling of electronic components.

## 2 Problem statement

Plotting of considered model (shown in fig. 1). It is a channel of height  $H = 40$  mm and length  $L = 520$  mm ( $13H$ ) containing two substrates of length  $L_p = 160$  mm ( $4H$ ), separated by a height  $S_p = 15$  mm ( $0.375H$ ). On each substrate is placed four blocks height  $h_p = 6$  mm ( $0.15H$ ) and width  $w_b = 20$  mm ( $0.5H$ ). The distance between two consecutive blocks is  $S_b = 20$  mm ( $0.5H$ ). The two Substrates are assumed adiabatic, while the blocks are submitted to heat generation per unit volume  $q_v$ .

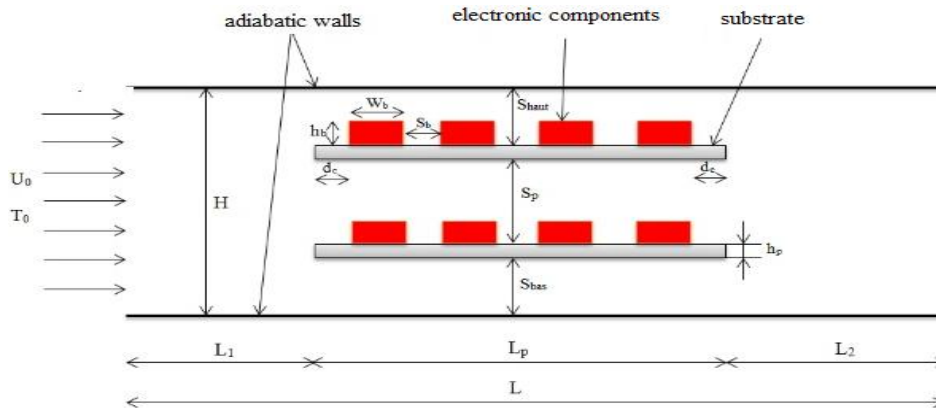


Figure 1: Scheme of the problem

## 3 Mathematical formulation

The study of a physical phenomenon requires the formulation of laws in the form of mathematical equations relating the different variables involved in the course of the phenomenon. In general, these equations are: the continuity equation which expresses the principle of conservation of mass, the Navier-Stokes equations which express the principle of conservation of momentum and energy equation represents the principle of

energy conservation.

### 3.1 Simplifying assumptions

In order to simplify the resolution of mathematical equations describing the present physical model, the following hypotheses are considered:

- The nanofluid is assumed incompressible and Newtonian.
- The flow is laminar, stationary and two-dimensional.
- The base fluid and nanoparticles are in thermal equilibrium state and no slip occurs between them.
- Radiation heat transfer is negligible compared with other modes of heat transfer.
- The shape of nanoparticles used in this paper is only spherical with diameter less than 10 nm because nanofluids containing spherical nanoparticles are more likely to exhibit Newtonian behavior and those containing nanotubes show non-Newtonian flow behavior.

### 3.2 Governing equations

It is noted that all the equations of conservation (mass, Momentum and energy) as well known for single-phase fluids can be directly extended and employed for nanofluids.

Mass conservation equation:

$$\frac{\partial u}{\partial x} + \frac{\partial v}{\partial y} = 0 \quad (1)$$

Conservation equation of momentum:

$$u \frac{\partial u}{\partial x} + v \frac{\partial u}{\partial y} = -\frac{1}{\rho_{nf}} \times \frac{\partial p}{\partial x} + \frac{\mu_{nf}}{\rho_{nf}} \left( \frac{\partial^2 u}{\partial x^2} + \frac{\partial^2 u}{\partial y^2} \right) \quad (2)$$

$$u \frac{\partial v}{\partial x} + v \frac{\partial v}{\partial y} = -\frac{1}{\rho_{nf}} \times \frac{\partial p}{\partial y} + \frac{\mu_{nf}}{\rho_{nf}} \left( \frac{\partial^2 v}{\partial x^2} + \frac{\partial^2 v}{\partial y^2} \right) \quad (3)$$

Energy equation:

$$u \frac{\partial T}{\partial x} + v \frac{\partial T}{\partial y} = \alpha_{nf} \left( \frac{\partial^2 T}{\partial x^2} + \frac{\partial^2 T}{\partial y^2} \right) + q_v \quad (4)$$

**With:**

$$\alpha_{nf} = \frac{k_{nf}}{(\rho C_p)_{nf}} \quad (5)$$

### 3.3 Thermo-physical properties of nanofluid

Adding nanoparticles to the base fluids modifies considerably their thermophysical properties, so to calculate the properties of nanofluids we use the following formulas:

The volume fraction of the nanoparticles is given as:

$$\varphi = \frac{V_s}{V_s + V_f} \quad (6)$$

The density of nanofluid is given by:

$$\rho_{nf} = (1 - \varphi)\rho_f + \varphi\rho_s \quad (7)$$

The dynamic viscosity according to the [Brinkman (1952)] model is given as:

$$\mu_{nf} = \frac{\mu_f}{(1 - \varphi)^{2.5}} \quad (8)$$

The specific heat and thermal expansion according to [Khanafar, Vafai & Lightstone (2003)] model are given by:

$$(\rho C_p)_{nf} = (1 - \varphi)(\rho C_p)_f + \varphi(\rho C_p)_s \quad (9)$$

$$(\rho\beta)_{nf} = (1 - \varphi)(\rho\beta)_f + \varphi(\rho\beta)_s \quad (10)$$

The effective thermal conductivity according to the model of [Hamilton Crosser (1969)]:

$$\frac{k_{nf}}{k_f} = \frac{k_s + (1 - n)k_f + (n - 1)\varphi(k_f - k_s)}{k_s + (1 - n)k_f + \varphi(k_f - k_s)} \quad (11)$$

$$\text{With: } n = \frac{3}{\psi}$$

For  $\psi = 1$  (spherical particles) Hamilton model is similar to [Maxwell-Garnetts (1873)] model. The effective thermal conductivity according to this model:

$$\frac{k_{nf}}{k_f} = \frac{k_s + 2k_f - 2\varphi(k_f - k_s)}{k_s + 2k_f + \varphi(k_f - k_s)} \quad (12)$$

There are other models that take into account the Brownian motion such as [Chon, Kihm, Lee and choi (2005)] model:

$$k_{nf} = k_{bf} \left[ 1 + 64.7\varphi^{0.746} \left( \frac{d_{bf}}{d_p} \right)^{0.369} \left( \frac{k_p}{k_{bf}} \right)^{0.7476} \text{Pr}^{0.9955} \text{Re}^{1.2321} \right] \quad (13)$$

In this study, we use the Maxwell-Garnetts model, because the shape of nanoparticles is spherical. This model does not account for others shapes of nanoparticles (i.e. cylindrical and square...).

### 3.4 Dimensionless governing parameters

The study of the forced convection flow require the setting up of dimensionless parameters, namely the flow Reynolds number, the Prandtl number and the dimensionless thermal conductivity and dynamic viscosity.

The following dimensionless groups are introduced:

$$X = \frac{x}{H}; \quad Y = \frac{y}{H}; \quad U = \frac{u}{u_0}; \quad V = \frac{v}{u_0}; \quad \theta = \frac{T - T_0}{\Delta T}; \quad \Delta T = \frac{q_v H^2}{k_f} \quad (14)$$

By using the dimensionless parameters the equations are written as:

Mass conservation equation:

$$\frac{\partial U}{\partial X} + \frac{\partial V}{\partial Y} = 0 \quad (15)$$

Conservation equation of momentum:

$$U \frac{\partial U}{\partial X} + V \frac{\partial U}{\partial Y} = -\frac{\partial P}{\partial X} + \frac{\mu_{nf}}{\rho_{nf} \nu_f} \frac{\nu^*}{\text{Re}} \left( \frac{\partial^2 U}{\partial X^2} + \frac{\partial^2 U}{\partial Y^2} \right) \quad (16)$$

$$U \frac{\partial V}{\partial X} + V \frac{\partial V}{\partial Y} = -\frac{\partial P}{\partial Y} + \frac{\mu_{nf}}{\rho_{nf} \nu_f} \frac{\nu^*}{\text{Re}} \left( \frac{\partial^2 V}{\partial X^2} + \frac{\partial^2 V}{\partial Y^2} \right) \quad (17)$$

Energy equation:

- For the fluid:

$$U \frac{\partial \theta}{\partial X} + V \frac{\partial \theta}{\partial Y} = k_{nf}^* \times \frac{1}{\text{Re Pr}} \left( \frac{\partial^2 \theta}{\partial X^2} + \frac{\partial^2 \theta}{\partial Y^2} \right) \quad (18)$$

- For the substrates:

$$\frac{k_s^*}{\text{Re Pr}} \left( \frac{\partial^2 \theta}{\partial X^2} + \frac{\partial^2 \theta}{\partial Y^2} \right) = 0 \quad (19)$$

- For the blocks:

$$\frac{k_b^*}{\text{Re Pr}} \left( \frac{\partial^2 \theta}{\partial X^2} + \frac{\partial^2 \theta}{\partial Y^2} \right) + \frac{1}{\text{Re Pr}} = 0 \quad (20)$$

With:

$$k^* = \frac{k}{k_f} = \begin{cases} \text{finite on each block} \\ 1 \text{ on fluid} \end{cases} \quad (21)$$

$$\nu^* = \frac{\nu}{\nu_f} = \begin{cases} \infty \text{ on each block} \\ 1 \text{ on fluid} \end{cases} \quad (22)$$

### 3.5 Boundary conditions

In fact, most of heat transfer flow problems have a similar governing equations of conservation (mass, momentum and energy) but, different final solutions, this is mainly due to the difference of the boundary conditions and physical properties of fluids

The dimensionless boundary conditions are written as:

On the walls of channel:

$$U = 0; \quad V = 0; \quad \frac{\partial \theta}{\partial Y} = 0 \quad (23)$$

At the inlet of the channel:

$$U = 1; \quad V = 0; \quad \theta = 0 \quad (24)$$

At the outlet of channel:

On the substrates:

$$U = 0; \quad V = 0; \quad \frac{\partial \theta}{\partial N} = 0 \quad (25)$$

On the blocks:

$$U = 0; \quad V = 0 \quad (26)$$

It is noted that the blocks are also subject to a volumetric heat generation  $q_v$

Condition at the solid-fluid interface:

$$\left( -K^* \frac{\partial \theta}{\partial N} \right)_{nf} = \left( -K^* \frac{\partial \theta}{\partial N} \right)_s \quad (27)$$

### 3.6 Nusselt number

The local variation of the Nusselt number of the fluid can be expressed as:

$$Nu = - \left( \frac{K_{nf}}{K_f} \right) \frac{\partial \theta}{\partial N} \Big|_{ABCD} \quad (28)$$

The average Nusselt number is defined by:

$$\overline{Nu} = \frac{1}{AB + BC + CD} \int_{ABCD} Nu \, dN \quad (29)$$

The number of total average Nusselt is defined by:

$$\overline{Nu}_t = \sum_{i=1}^8 \overline{Nu}_i \quad (30)$$

## 4 Numerical method and grid sensitivity study

The motion and energy equations subject to the boundary conditions described previously are discretized by adopting a numerical method based fundamentally on the 'finite

control volume approach'. developed by [Patankar (1980)]. This method, as other members of the SIMPLE-code family is based on following two principals steps, the first is the integration of a generic transport equation of the quantity  $\Phi$  over a control volume. The second, is the discretization i.e. the numerical solution will require that we need to transform it into an algebraic equation, COUPLED algorithm is used to deal with the problem of velocity and pressure coupling. The diffusion term in the momentum and energy equations is approximated by the first-order central difference which gives a stable solution. Before proceeding to the calculations of our study, we examined the influence of the mesh on the numerical solution, five different sets of the grid size were imposed to the geometry and simulated by calculating the average Nusselt number on each component, the dimensionless axial and vertical velocity and dimensionless temperature for  $Re=10$ , volume fraction of copper nanoparticles  $\phi=0.03$  and  $K_s^*=400$ , the five grids sizes are  $241 \times 61$ ,  $261 \times 81$ ,  $281 \times 161$ ,  $301 \times 121$  and  $321 \times 141$  corresponding respectively to 14701, 21141, 28381, 36421 and 45261 nodes. The accuracy of results depends on the mesh size used. The numerical solution converges to the real solution when the variation of mesh has not more influence on the solution; otherwise convergence is reached when the error between two consecutive solutions tends to zero. To satisfy this criterion, a sensitivity analysis to the mesh was performed, as shown in table 1 and figure 2, giving respectively the values of the average Nusselt number in each component, and the maximum of velocities and temperature within the channel, and local Nusselt number at the fourth component of the upper substrate, show that the differences between numerical solutions corresponding to Grid (G4) and (G5) are insignificant, and for a good compromise between accuracy results and computation time we opted for the grid  $G4 = 36421$ .

**Table 1:** Effect of the mesh on numerical solution

<b>Grid nodes</b>	<b>G1</b>	<b>G2</b>	<b>G3</b>	<b>G4</b>	<b>G5</b>
$\overline{Nu}_1$	10.218	10.210	10.210	10.226	10.222
$\overline{Nu}_2$	6.944	6.955	6.963	6.970	6.970
$\overline{Nu}_3$	5.422	5.419	5.427	5.433	5.433
$\overline{Nu}_4$	4.456	4.456	4.462	4.468	4.468
$\overline{Nu}_5$	10.279	10.271	10.272	10.287	10.287
$\overline{Nu}_6$	7.019	7.013	7.019	7.026	7.026
$\overline{Nu}_7$	5.477	5.473	5.479	5.485	5.485
$\overline{Nu}_8$	4.504	4.503	4.508	4.515	4.515
$U_{max}$	2.128	2.145	2.149	2.149	2.153
$V_{max}$	0.722	0.726	0.739	0.735	0.743
$\theta_{max}$	0.0207	0.0208	0.0208	0.0208	0.028

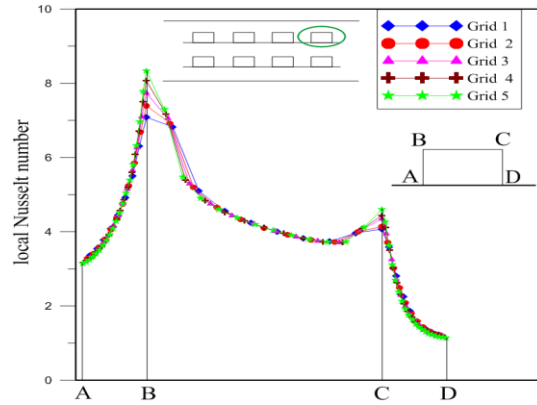


Figure 2: Local nusselt number along the interface of blocks for the five grids.

#### 4.1 Code validation

In order to give more credibility to the present work, it is necessary to achieve a validation of computer code, comparing the results obtained with those of a previous study.

The validation was performed on a study conducted by [Pishkar and Ghasemi (2012)], who studied mixed convection in a horizontal channel in the presence of two conductive fins simulating electronic components on the bottom wall kept at a constant temperature ( $T_h = 303K$ ), using a nanofluid (water + copper nanoparticles) as shown in fig.2 for a Richardson number ( $Ri = 10$ ), a volume fraction ( $\varphi = 0.03$ ), and vas Reynolds number. The comparison results are shown in Figures below.

The analysis of velocity profiles, temperature contours obtained through various simulation show good qualitative and quantitative agreement with those obtained by Pishkar and Ghasemi.

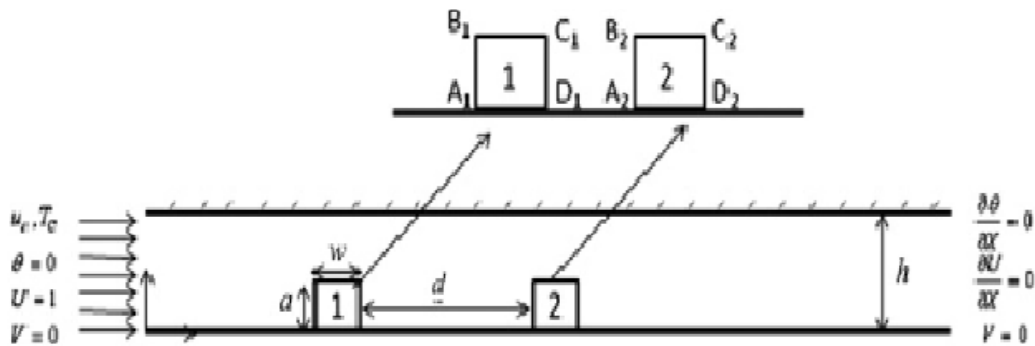
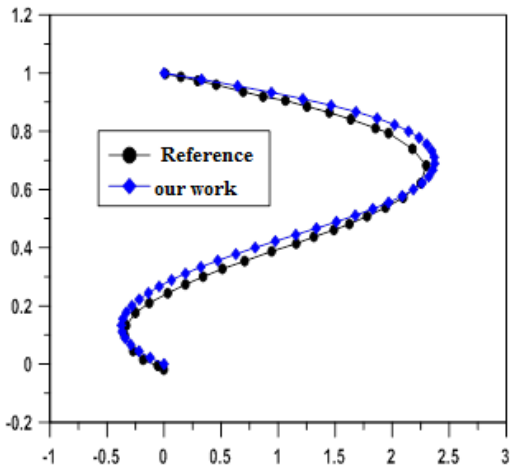
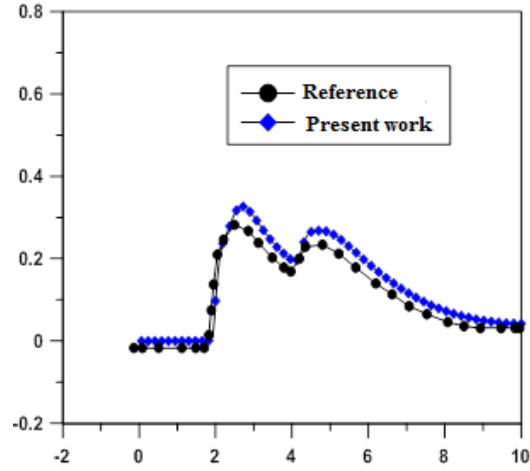


Figure 3: Geometry of pishkar and ghasemi study



**Figure 4:** The horizontal velocity profile  $U$  as a function of  $Y$  for  $X=3.25$  and  $Re=100$



**Figure 5:** Profile of dimensionless temperature as function of  $X$  for  $Y=0.5$  and  $Re=100$

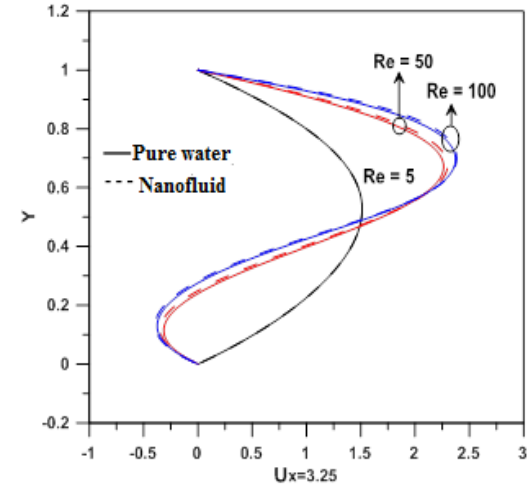
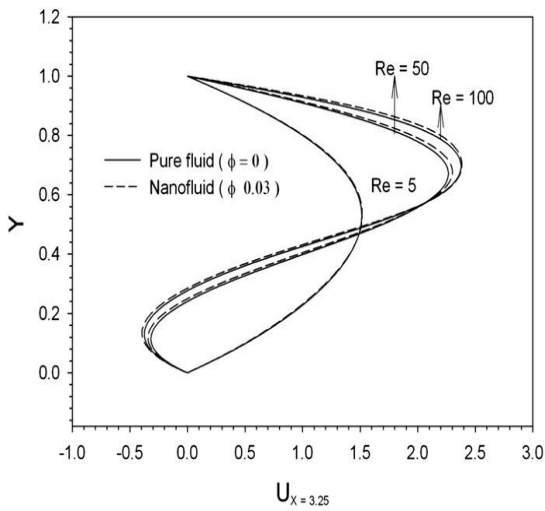


**Figure 6:** Profile of horizontal velocity  $U$  according to  $Y$  (results Ghasemi and Pishkar On the left and our results on the right).

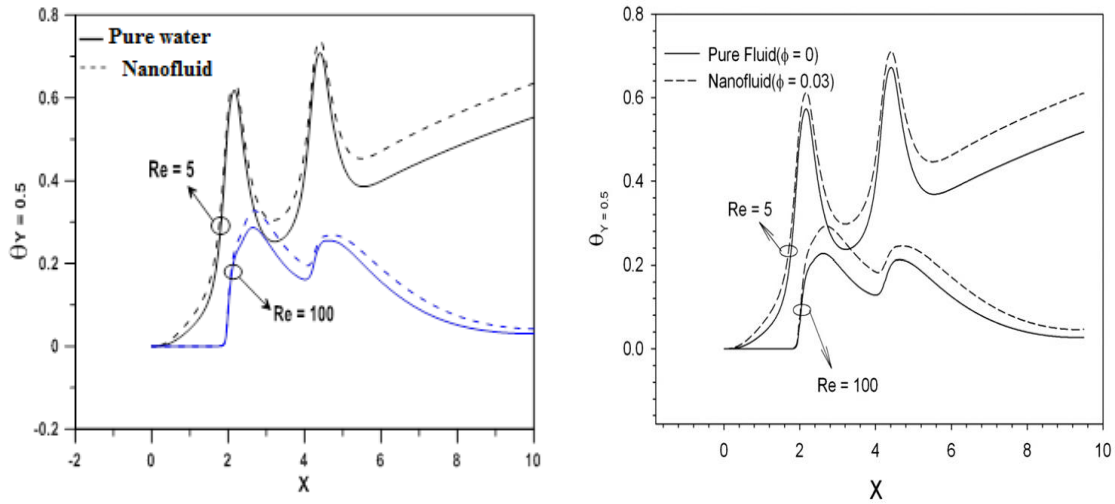


**Figure 7:** Dimensionless temperature profile function of  $X$  (results Ghasemi and Pishkar on the right and our results on the left).

## 5 Results and discussion

The simulations were performed of laminar forced convective heat transfer and fluid flow through a channel with four different types of nanofluids such as  $\text{Al}_2\text{O}_3$ , Cu,  $\text{SiO}_2$ , Ag and diamond with pure water as a base fluid. Four values of Reynolds number were used in the range of  $10 \leq \text{Re} \leq 500$  with six nanoparticles volume fraction in the range of  $0 \leq \varphi \leq 0.2$ . The effects of Reynolds number, volume fraction nanoparticle type with the same base fluids on dynamic and thermal fields of flow the Nusselt number are analyzed and discussed in this section.

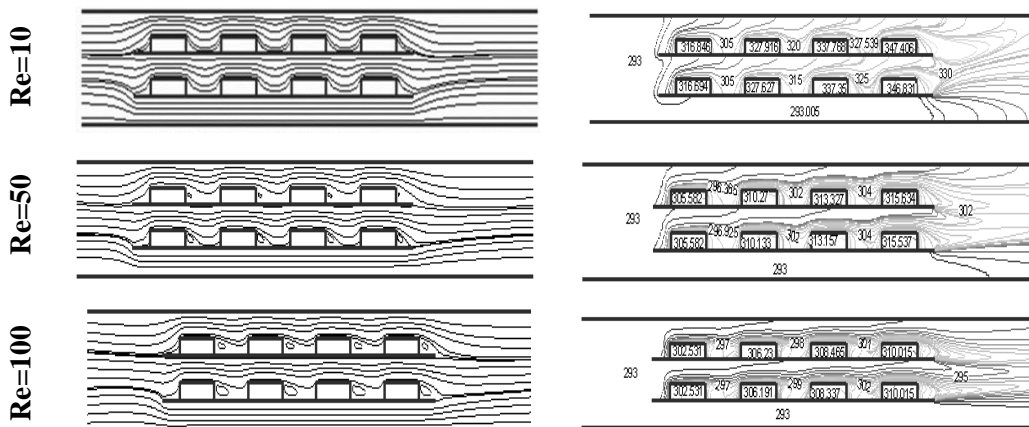
### 5.1 Effect of reynolds number

In order to examine the effect of Reynolds number on the hydrodynamic and thermal field flow, a numerical simulations were performed for a volume fraction of copper nanoparticles ( $\varphi = 0.03$ ), thermal conductivity dimensionless ( $K_s^* = 400$ ) and for different Reynolds numbers. Fig.8 shows the evolution of stream functions on the left and isotherms on the right. It is noted that for  $\text{Re} = 10$ , there is no recirculation zones between the blocks and on downstream of the last block. This is due to low inertial forces compared to viscous forces, which slowing the movement of the fluid because the speed imposed to entry of channel is very low. The fluid moves by crawling essentially adjacent blocks. By increasing the Reynolds number gradually the velocity of the fluid increases which allows the increase of inertial forces. For  $\text{Re} = 50$  we see the beginning of formation of recirculation zones in the vicinity of the blocks. By further increasing the Reynolds number for 100 and 500, it is noted that the size of recirculation zones increases considerably. This can be explained by the fact that the inertial forces imposed have a

reducing effect of viscous forces that remain constant in this case. In addition to the stream function, the effect of the Reynolds number on the shape of isotherms is significant as shown in Fig.8. For  $Re = 10$ , we note that the isotherms extend and occupy much of the geometry. They form an important thermal boundary layer in the vicinity of the blocks. For high values of Reynolds number ( $Re = 50, 100, 500$ ), the isotherms are tightened because of the increase in velocity of the fluid upstream of the blocks. The isothermal expansion is further reduced while the increasing of Reynolds number essentially at the block. These isotherms tend to become horizontal, with a significant decrease in thermal boundary layer. It is thus found that the temperature at the component decreases with increasing Reynolds number.

In order to evaluate the intensity of heat exchange quantitatively, a detailed description on the heat transfer rate is shown in the Fig.9 which show the profile of local Nusselt number along the interfaces of all blocks for  $Re = 10$  on the top and  $Re=100$  on the bottom. It is noted that the profile of local Nusselt number decreases from the first to the fourth and the fifth to eighth component. It is clear from these profiles that the maximum of heat transfer is observed in the upper left corner of each component [Kim, Sung and Sung (1992)]. Note also that the heat transfer is better for the first and the fifth component particularly on the sides AB and BC. By increasing the Reynolds number of  $Re = 10$  to  $Re = 100$ , there is a significant improvement in the heat transfer rate.

For a better interpretation of the results obtained during the simulations it is preferable to analyze the evolution of the average Nusselt number on each component for different Reynolds numbers, as shown in Fig. 10. It is noted that the average Nusselt number increases while increasing of Reynolds number and this is valid for all components especially the fifth and the first component which have a high proportionality between the Reynolds number and the average Nusselt number. It remains to say that the overall transfer rate represented by the total Nusselt number of eight components is gradually improving for increasing Reynolds numbers as shown in Fig. 11.



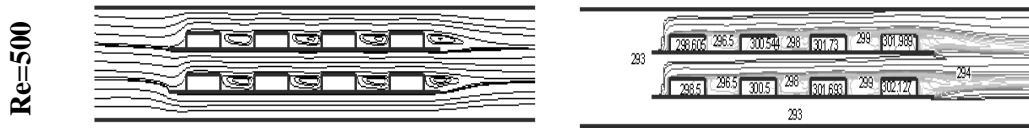


**Figure 8:** Contour of stream function on the left and isotherms on the right, for different values of Reynolds number.

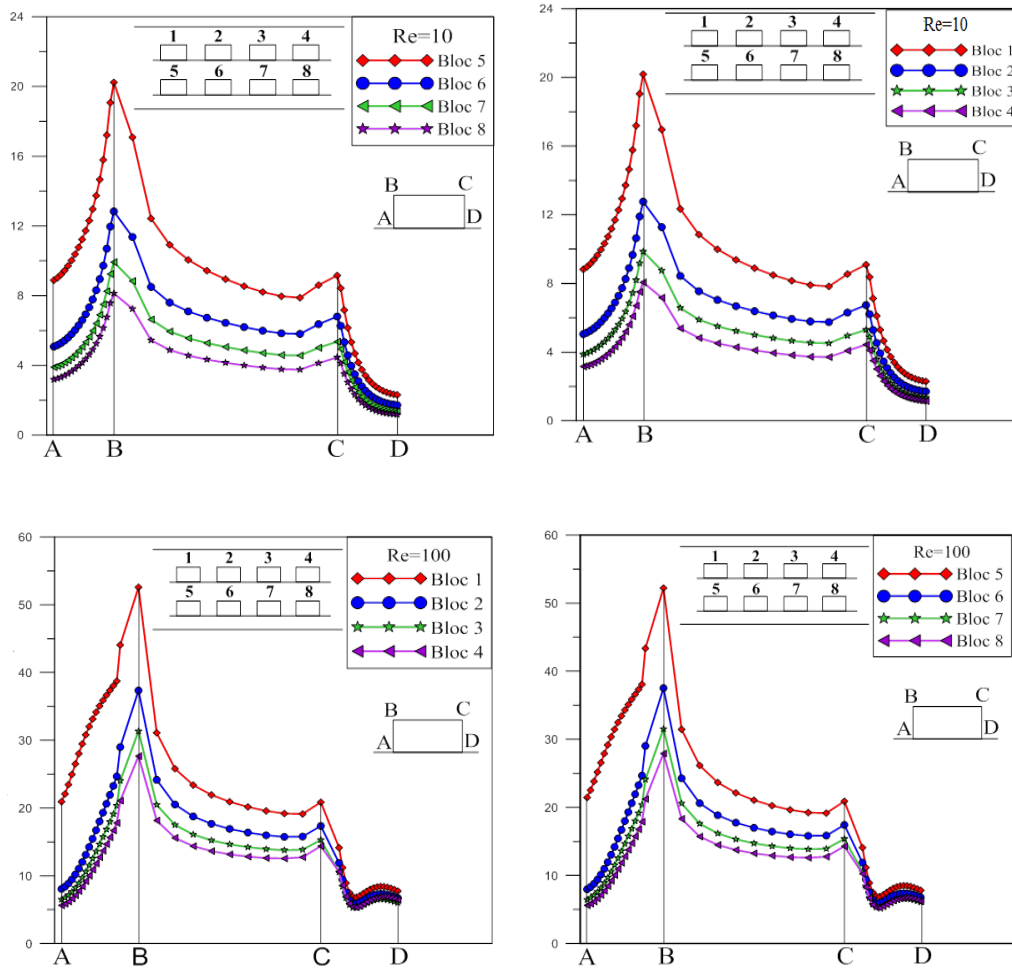


**Figure 9:** Local Nusselt number (Nu) along the interfaces of all blocks for  $Re = 10$  on the the bottom for  $\varphi = 0.03$  and  $K_s^* = 400$

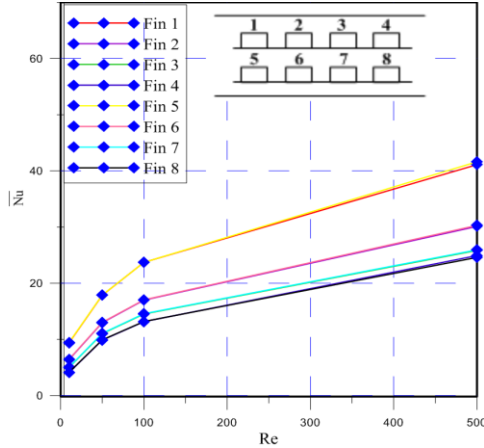


**Figure 10:** Average Nusselt number against Reynolds number

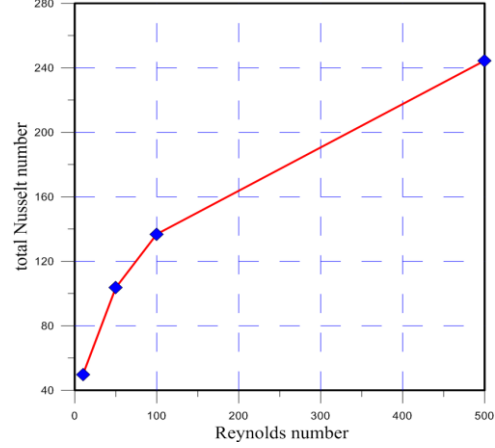


**Figure 11:** Total Nusselt number against Reynolds number for the eight blocks.

**5.2 Effect of the volume fraction of the nanoparticles**

To examine the influence of the volume fraction  $\phi$  of nanoparticles on the dynamic and thermal field of flow, numerical simulations were made for the fixed Reynolds number ( $Re = 100$ ) and for the dimensionless thermal conductivity ( $K_s^* = 400$ ). The nanofluid used is the (Cu-Water), for different volume fractions in the range of  $0 \leq \phi \leq 0.2$ .

The consultation of fig.12 showing the contours of stream function for different concentration of nanoparticles, it is noted that the variation of the volume fraction of the nanoparticles does not have a great effect on the structure of the flow, except the increase in recirculation zones while increasing the volume fraction. This is due to the presence of the nanoparticles, which leads to an increase of the effective conductivity, and consequently the greater absorption of heat from heat sources. It is evident that increasing the volume fraction develops recirculation zones which the increase in size is due to the forced flow Induced by contact with the vertical faces of the heat sources. This contact provides improved heat transfer at all surfaces. In order to assess the effect of varying the volume fraction on the dynamic field of flow, we have plotted the fig.13 representing the dimensionless velocity profile against Y in the section  $x=0.2m$  for different concentrations, we find that there are no significant changes in the velocity profiles, this can be explained by the fact that the dynamic field inside the channel is not affected by the increase in the volume fraction of nanoparticles, in other words the sedimentation effect is almost negligible for these values of volume fraction. For purposes of describing the thermal field of flow we plot the Fig.12 right side and fig.14 representing respectively the contour of isotherms and dimensionless temperature profile for different concentrations of nanoparticles, just as the stream functions, the change in the concentration does not have a great effect on the shape of isotherms, this can be

explained by a low intensity of convection within the channel. However, the Fig.14 shows that the nanofluid is better for cooling electronic components, compared with pure water and the cooling efficiency increases with the concentration of the nanoparticles. The fig. 15 shows the variation of local Nusselt number along the interfaces of components on the upper substrate (components 1, 2, 3, 4) corresponding to the volume fraction  $\phi = 0$  (pure water),  $\phi = 0.03$  and  $\phi = 0.2$ , it is noted that the heat transfers are favorable for the first two components especially on the face (AB) and this is true for pure water and for different nanofluids, it is also noted that the local Nusselt number increases with the volume fraction on all interfaces of the blocks, which due mainly to improved thermophysical properties of nanofluid in particular its thermal conductivity which increases with the concentration of nanoparticles and by the flow induced by forced contact with the faces of the heat sources.

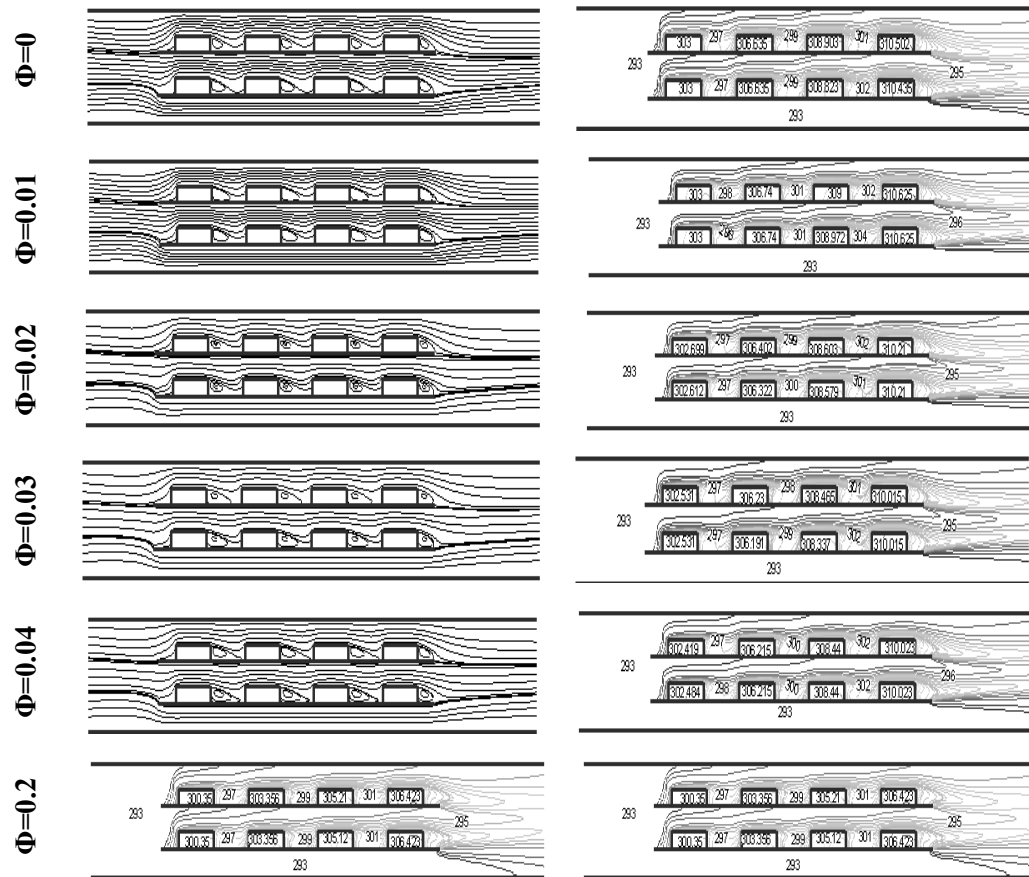


**Figure 12:** Contour of stream function on the left and isotherms on the right, for different volume concentration ( $\phi$ ).

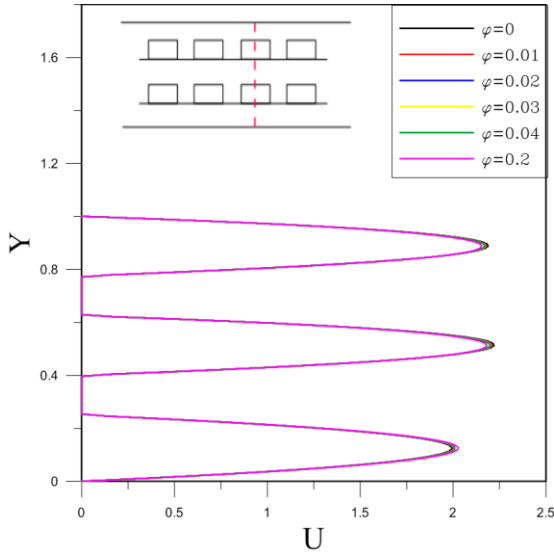


**Figure 13:** Dimensionless velocity profile for different volume fractions for  $x=0.2$  m,  $Re = 100$ ,  $K_s^* = 400$ .

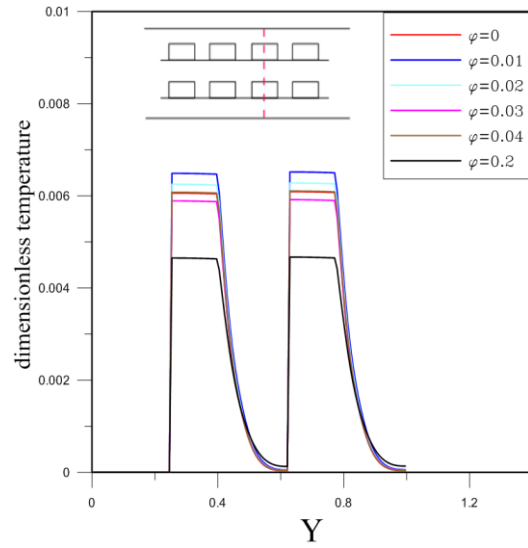


**Figure 14:** Dimensionless temperature profile for different volume fractions for  $x=0.2$  m,  $Re = 100$ ,  $K_s^* = 400$ .

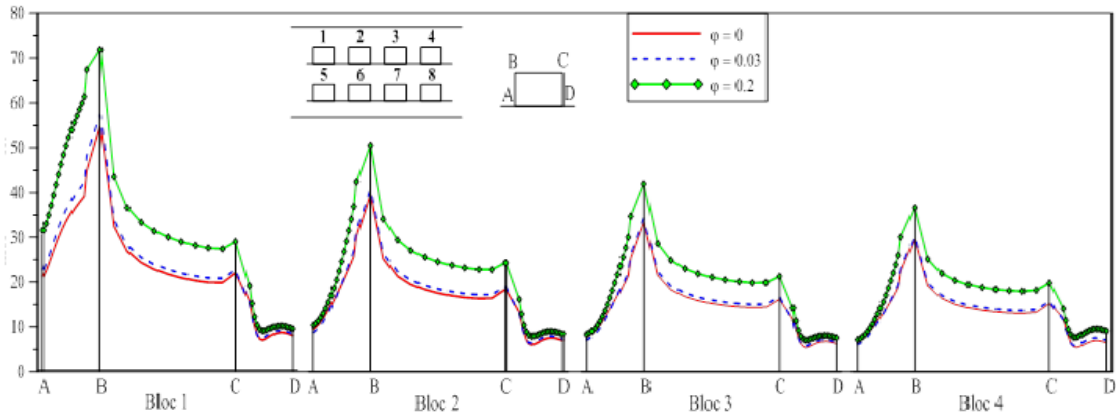


**Figure 15:** Local Nusselt number for different volume fractions along the block interfaces for  $Re = 100$ ,  $K_s^* = 400$ .

### 5.3 Effect of change in the type of nanoparticles

In order to know if the cooling of electronic components can be improved by changing the type of nanoparticles, our simulations were performed for the following nanoparticles: Cu,  $Al_2O_3$ ,  $SiO_2$ , Ag and diamond. For a Reynolds number ( $Re = 100$ ), all of

nanoparticles having the same volume fraction of 3% relative to its base fluid (pure water). The thermophysical properties of different nanoparticles used are shown in the table below.

**Table 2:** Thermophysical properties of different nanoparticles.

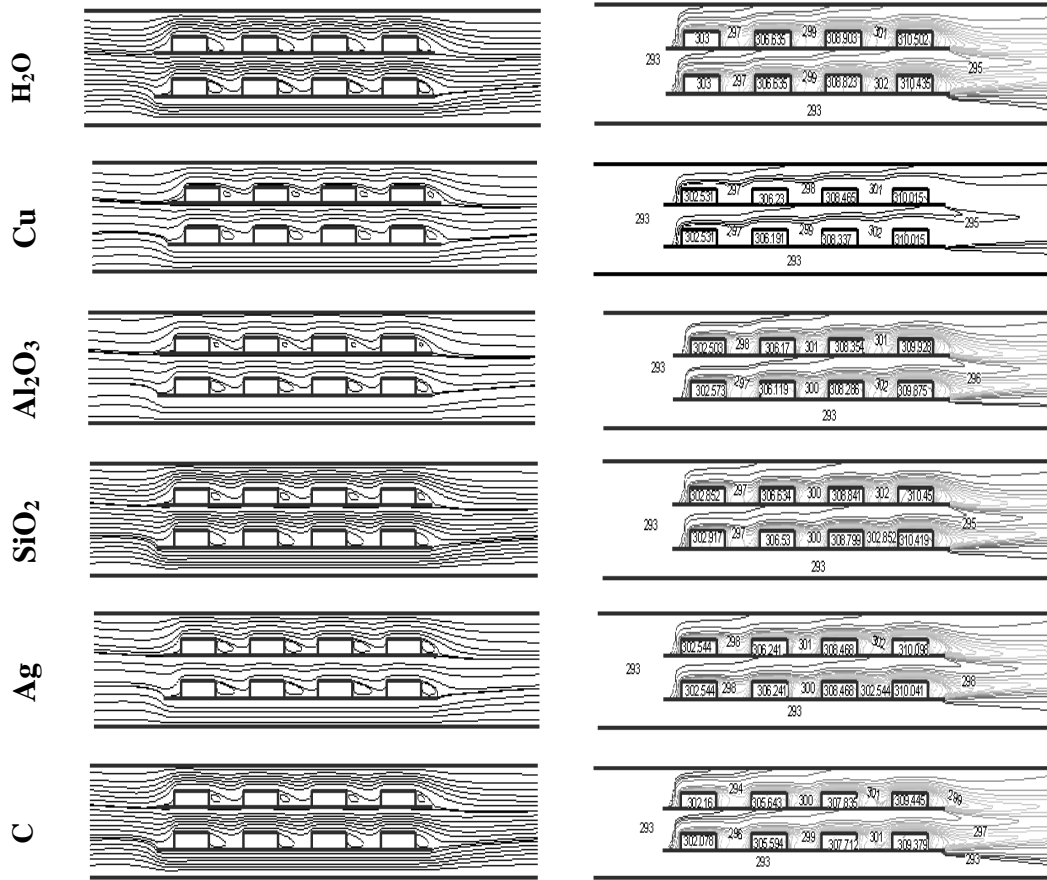
	Thermophysical properties	$C_p$ (J kg <sup>-1</sup> K <sup>-1</sup> )	$\rho$ (kg m <sup>-3</sup> )	$k$ (Wm <sup>-1</sup> K <sup>1</sup> )
Nanoparticles	Copper	385	8933	401
	aluminum oxide	761.55	3970	40
	Silicon dioxide	745	2220	1.4
	Silver	230	10500	418
	Diamond	502	3510	2000
	Pure water	4179	997.1	0.613

The dynamic field of flow is illustrated in fig.16 left side representing the contour of the stream functions for pure water and different nanofluids, shows that the size of the recirculation zones for nanofluids is reduced slightly compared to the base fluid, this reduction is observed especially for copper nanoparticles, diamond and aluminum oxide. And the fig.18 representing the distribution of the dimensionless velocity  $U = f(Y)$  in the section  $x = 0.2$  m, it is noted that the dynamic field remains almost insensitive to the change of nanoparticles type.

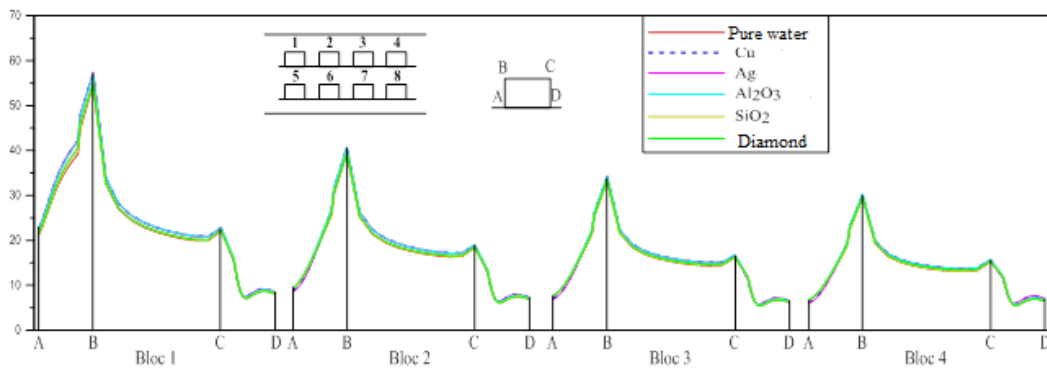
In an effort to examine the impact of the change of nanoparticles added to the base fluid (pure water in our case) on the thermal field of flow, we traced the fig.3 showing the isotherms for different nanoparticles. It is noted that the isotherms are not affected by the variation of nanofluid type so; there is a conservation of the shape and intensity of the isotherms. The lowest temperature at the components is recorded using the diamond-water, in that it has remarkable thermo physical properties in particular its thermal conductivity is larger compared to that of pure water and other nanofluids.

To evaluate the extent of the heat exchanges at the level of each component, the fig.17 shows the evolution of local Nusselt number for all nanofluids used, it is noted that the rate and heat transfer quality is significantly improved during the use the nanofluids compared to the base fluid (pure water).

The fig.19 represents the evolution of the average Nusselt number on all components for different nanofluids,  $\phi = 0.03$ ,  $Re = 100$  and  $K_s^* = 400$ . It is noted that there is a significant increase in the average Nusselt number during the use of nanofluids, this increase is most notable for (Cu-water) and (Al<sub>2</sub>O<sub>3</sub>-water) compared to other nanofluids particularly in components 1 and 5 because they are more exposed to the flow, so it can be concluded that the copper-water and oxide aluminum nanofluids are the best cooling agents for this study.



**Figure 16:** Contour of stream function on the left and isotherms on the right, for different values of Reynolds number.



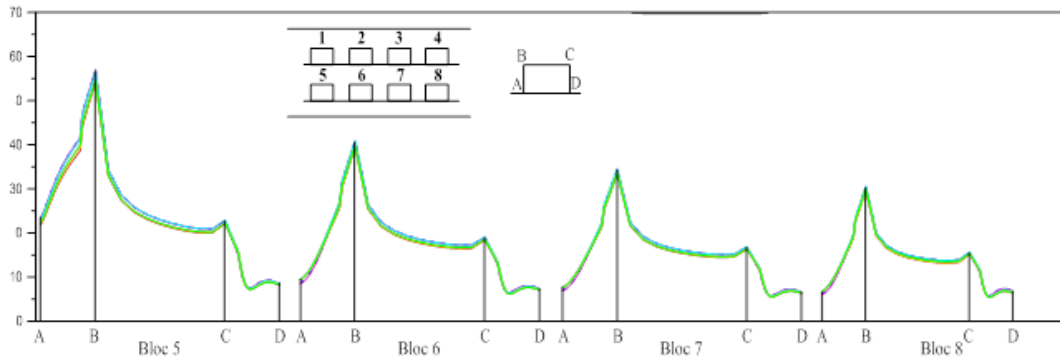


**Figure 17:** Local Nusselt number along the block interfaces for different nanofluids,  $\phi = 0.03$ ,  $Re = 100$  and  $K_s^* = 400$ .

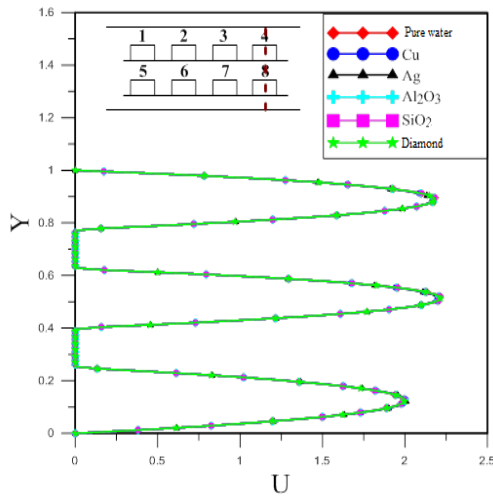


**Figure 18:** Dimensionless velocity profile for different nanoparticles for  $x = 0.2$  m  $\phi = 0.03$ ,  $Re = 100$  and  $K_s^* = 400$

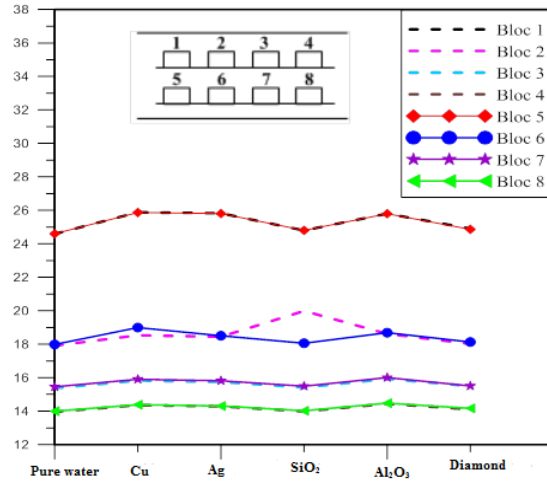


**Figure 19:** Average nusselt number on the interface of blocks for different nanoparticles,  $\phi = 0.03$ ,  $Re = 100$  and  $K_s^* = 400$ .

### 6 Conclusions

The study shows that the proper selection of certain parameters such as the Reynolds number, the volume fraction and a good choice of nanoparticles added to the base fluid causes a heat transfer enhancement, it is concluded that the use of the nanofluid presents a heat transfer rate much better than the base fluid in proportion to the volume fraction of nanoparticles knowing that not possible to increase it indefinitely in order to avoid sedimentation. Finally this investigation demonstrate that the (Al<sub>2</sub>O<sub>3</sub>-water) and (Cu-water) are considered as the best coolants.

**References**

- Akbari, M.; Behzadmehr, A.; Shahraki, F.** (2008): Fully developed mixed convection in horizontal and inclined tubes with uniform heat flux using nanofluid. *International Journal of Heat and Fluid Flow*, vol. 29, no. 2, pp. 545–556, Apr. 2008.
- Brinkman, H.C.** (1952): The viscosity of concentrated suspensions and solution. *The Journal of Chemical Physics*, vol.20, pp. 571-581.
- Choi, U.S.** (1995): Enhancing thermal conductivity of fluids with nanoparticles, Developments and application of non-Newtonian flows. *ASME*, vol. 66, pp. 99–105.
- Chon, C. H.; Kihm, K. D.; Lee, S. P.; Choi, S.U.S.** (2005): Empirical correlation finding the role of temperature and particle size for nanofluid ( $\text{Al}_2\text{O}_3$ ) thermal conductivity enhancement. *Applied Physics Letters*. 87: 153107.
- Elmir, M.; Mehdaoui, R.; Mojtabi, A.** (2012): Numerical Simulation of Cooling a Solar Cell by Forced Convection in the Presence of a Nanofluid. *Energy Procedia*, vol. 18, pp. 594–603, 2012.
- Hajipour, M.; Molaie Dehkordi, A.** (2014): Mixed-convection flow of  $\text{Al}_2\text{O}_3\text{-H}_2\text{O}$  nanofluid in a channel partially filled with porous metal foam: Experimental and numerical study. *Experimental Thermal and Fluid Science*, vol. 53, pp. 49–56, Feb.
- Hamilton, R.L.; Crosser, O.K.** (1969): *Thermal conductivity of heterogeneous systems*. *Ind. Engng Chem*, vol 1 (3), 1969, pp 187-191.
- Hussein, A. M.; Bakar, R. A.; Kadirgama, K.** (2014): Study of forced convection nanofluid heat transfer in the automotive cooling system. *Case Studies in Thermal Engineering*, vol. 2, pp. 50–61, Mar. 2014.
- Izadi, M.A.; Behzadmehr; Jalali-Vahida, D.** (2009): Numerical study of developing laminar forced convection of a nanofluid in an annulus. *International Journal of Thermal Sciences*, vol. 48, no. 11, pp. 2119–2129, Nov. 2009. Oct. 2012.
- Khanafar, K. K.; Vafai; Lightstone, M.** (2003): Buoyancy-driven heat transfer enhancement in a two-dimensional enclosure utilizing nanofluids. *International Journal of Heat and Mass Transfer*, vol. 46, no. 19, pp. 3639–3653, Sep. 2003.
- Kherbeet, A. S.; Mohammed, H. A.; Salman, B. H.** (2012): The effect of step height of microscale backward-facing step on mixed convection nanofluid flow and heat transfer characteristics. *International Journal of Heat and Mass Transfer*, vol. 68, pp. 554–566, 2014.
- Khedkar, R. S.; Sonawane, S. S.; Wasewar, K. L.** (2013): Water to nanofluids heat transfer in concentric tube heat exchanger: Experimental study. *Procedia Engineering*, vol. 51, no. NUiCONE 2012, pp. 318–323, 2013.
- Kim, S. Y.; Sung, H. J.; Hyun, J. M.** (1992): *Mixed convection from multiple-layered boards with cross-* 2941–2952, Nov. 1992.
- Mahmoudi, A. H.; Shahi, M.; Talebi, F.** (2010): Effect of inlet and outlet location on the mixed convective cooling inside the ventilated cavity subjected to an external nanofluid. *International Communications in Heat and Mass Transfer*, vol. 37, no. 8, pp. 1158–1173, Oct. 2010.2014.18, pp. 594–603, 2012.and *Mass Transfer*, vol. 68, pp. 78–84,

Jan. 2014.

**Maxwell, J.C.** (1873): *A Treatise on Electricity and Magnetism*, vol. II, Oxford University Press, Cambridge, UK, pp. 54.

**Mehrizi, A. A.; Farhadi, M.; Afroozi, H. H.; Sedighi, K.; Darz, A. A. R.** (2012): Mixed convection heat transfer in a ventilated cavity with hot obstacle: Effect of nanofluid and outlet port location. *International Communications in Heat and Mass Transfer*, vol. 39, no. 7, pp. 1000–1008, Aug. 2012.

**Minea, A. A.** (2014): Uncertainties in modeling thermal conductivity of laminar forced convection heat transfer with water alumina nanofluids. *International Journal of Heat and Mass Transfer*, vol. 68, pp. 78–84, Jan. 2014. *Engineering*, vol. 2, pp. 50–61, Mar.

**Patankar, S. V.** (1980): *Numerical Heat Transfer and Fluid Flow*, Hemisphere, Washington, DC.

**Parametthanuwat, T.; Bhuwakietkumjohn, N.; Rittidech, S.; Ding, Y.** (2015):

Experimental investigation on thermal properties of silver nanofluids. *International Journal of Heat and Fluid Flow*, vol. 56, pp. 80–90, 2015.

**Pishkar, I.; Ghasemi, B.** (2012): Cooling enhancement of two fins in a horizontal channel by nanofluid mixed convection. *International Journal of Thermal Sciences* 59 (2012) 141e151.

**Shahi, A. H. Mahmoudi, and F. Talebi.** (2009): Numerical study of mixed convective cooling in a square cavity ventilated and partially heated from the below utilizing nanofluid. *International Communications in Heat and Mass Transfer*, vol. 37, no. 2, pp. 201–213, Feb. 2010.

**Yang, Y. T.; Lai, F.-H.** (2010): Numerical study of heat transfer enhancement with the use of nanofluids in radial flow cooling system. *International Journal of Heat and Mass Transfer*, vol. 53, no. 25–26, pp. 5895–5904, Dec. 2010.

**Zhang, P.; Hong, W.; Wu, J. F.; Liu, G. Z.; Xiao, J.; Chen, Z. B.; Cheng, H. B.** (2014): Effects of Surface Modification on the Suspension Stability and Thermal Conductivity of Carbon Nanotubes Nanofluids. *Energy Procedia*, vol. 69, pp. 699–705, 2015. *Journal of Heat and Fluid Flow*, vol. 56, pp. 80–90, 2015.